

SYNTHESIS, CHARACTERIZATION, AND REACTIVITY OF FEITKNECHTITE

J. Luo*, S. R. Segal*, J. Y. Wang*, Z. R. Tian*, S. L. Suib*,**

*U-60, Department of Chemistry, University of Connecticut
Storrs, CT 06269-4060, suib@uconnvm.uconn.edu

**Department of Chemical Engineering and Institute of Materials Science

ABSTRACT

The synthesis of Mg^{2+} doped β - $MnOOH$ which is known as feitknechtite is reported. Feitknechtite is a layered material having the CdI_2 structure. The characterization of Mg^{2+} doped feitknechtite was done with X-ray powder diffraction, elemental analysis, energy dispersive X-ray analysis, scanning electron microscopy, alternating current (AC) impedance, Fourier transform infrared spectroscopy, thermogravimetric analysis, differential scanning calorimetry, average oxidation state titrations of manganese, and acidity measurements. The formation of feitknechtite is related to the MnO_4^-/Mn^{2+} ratio used in the synthesis. Feitknechtite can be converted to synthetic birnessite or octahedral layer birnessite (OL-1) which is a precursor to the 6.9 Å tunnel structure material todorokite.

INTRODUCTION

The mineral feitknechtite [β - $MnOOH$] was first studied systematically by Feitknecht and Marti in 1945 [1]. They prepared a mixed phase of $MnOOH$ and Mn_3O_4 by oxidation of an aqueous suspension of $Mn(OH)_2$. They assigned this mixed phase material on the basis of X-ray powder diffraction methods and referred to it as hydrohausmannite. Frondel in 1952 reported [2] that a mineral from Franklin, New Jersey had a similar X-ray powder diffraction pattern as that of hydrohausmannite. In 1962, Feitknecht, Brunner, and Oswald [3] suggested on the basis of electron microscopy data that the material referred to as hydrohausmannite by Feitknecht and Marti [1] was a mixture of Mn_3O_4 and β - $MnOOH$, which was thereafter referred to as feitknechtite.

The structure of β - $MnOOH$ is now recognized as having the CdI_2 structure [4]. There are two other $MnOOH$ phases. All three phases consist of $MnO_3(OH)_3$ octahedra that share edges and vertices in different ways. One of the other two phases is α - $MnOOH$ which is known as groutite and has a double chain structure [4]. The other phase γ - $MnOOH$ is known as manganite and has a corrugated structure [4]. Different oxidation conditions can yield synthetic versions of manganite [5, 6]. Stability relationships among these and other phases have been discussed by Bricker [7]. The structures of all three phases are shown in Figure 1.

The goals of this research were to study the synthesis mechanism of Mg^{2+} doped synthetic birnessite which has been referred to as octahedral layer (OL-1);

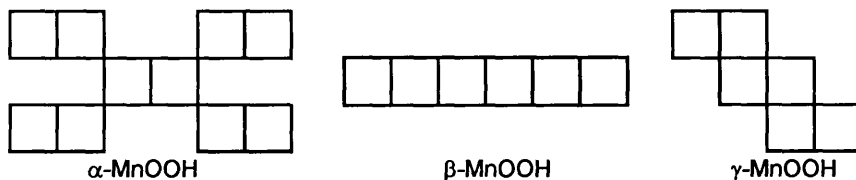


Figure 1. Structures of Various MnOOH Materials.

to understand the formation of feitknechtite [β -MnOOH]; to characterize synthetic feitknechtite; and to study the stability of feitknechtite. Feitknechtite is an octahedral layer structure which from herein will be referred to as OL-2. We have reported that the incorporation of Mg^{2+} into the framework structure of synthetic birnessite or OL-1 is critical in controlling the thermal stability of OL-1 as well as tunnel structure materials like synthetic todorokite (OMS-1) that can be prepared from OL-1 [8,9]. We report here the clean transformation of Mg^{2+} doped synthetic feitknechtite into OL-1.

EXPERIMENTAL SECTION

Synthesis of Mg^{2+} Doped Feitknechtite.

Feitknechtite was prepared by dissolving 20 g of NaOH in 80 mL of distilled deionized water (DDW). A second solution of 7.5 g $MnCl_2 \cdot 4H_2O$ and 1.5 g of $MgCl_2 \cdot 6H_2O$ in 50 mL of DDW is slowly mixed with the first solution and stirred for 20 min. An orange white precipitate is formed which is filtered, and washed with DDW in a centrifuge until the pH decreases to 10. The wet solid is then air dried at room temperature for a few minutes until a dark brown fine powder is produced.

Characterization.

X-ray powder diffraction patterns were collected on a Scintag XDS-200 diffractometer using Cu $K\alpha$ radiation and 45 kV and 40 mA. Scans were done at $5^\circ 2\theta$ per minute. Differential scanning calorimetry and thermogravimetric analyses were done as reported previously [8,9]. Procedures for elemental analysis [8,9], energy dispersive X-ray analysis [8,9], scanning electron microscopy [8,9], ac impedance [10], Fourier transform infrared spectroscopy [11], thermogravimetric analysis [8,9], differential scanning calorimetry [8,9], average oxidation state titrations of manganese [8,9], and acidity measurements have been reported previously, except for the following specific procedures. Samples were completely dissolved in aqua regia and diluted with DDW prior to atomic absorption analyses. All ac impedance measurements were done at low (1 kHz) frequency. Samples for acidity measurements were done on 10-20 mg pressed pellets that were thermally dehydrated to $150^\circ C$ at 5×10^{-5} torr for 3 h. Pyridine chemisorption was done at $100^\circ C$ for 30 min followed by heating to $140^\circ C$ for 3 h to remove physisorbed pyridine.

RESULTS

XRD data for Mg^{2+} doped synthetic feitknechtite show a major peak at 4.59 Å. This is assigned to the (002) reflection of feitknechtite. There are no other reported reflections for any manganese oxide, hydroxide or oxyhydroxide at this d-spacing. Two other reflections of feitknechtite are observed at 2.57 Å (311) and at 2.40 Å (312) which are the second and third most intense reflections. There are only 3 other very weak ($I = 10, 1, 1$) reflections reported for feitknechtite (JCPDS 18-804) which are not observed in our sample. These diffraction data are consistent with an octahedral layer structure which from herein will be referred to as OL-2.

If the synthesis is allowed to continue for 1.5 days, then reflections indicative of OL-1 are observed. Major peaks at 12.5° and 25° 2θ are observed as well as less intense peaks, all indicative of OL-1.

Average manganese oxidation state (AMOS) titration data for OL-2 suggest an oxidation state of 3.15. This value is significantly lower than other octahedral layer materials like OL-1 with an AMOS = 3.6 and octahedral molecular sieves having tunnel structures like synthetic cryptomelane (OMS-2) with an AMOS = 3.9, and synthetic todorokite (OMS-1) with an AMOS = 3.6.

Elemental analyses yield an overall formula of $Na_{0.3}Mg_{0.3}(OH)_{0.9}MnOOH$. Such data show that Mg^{2+} is present @ 6.5% and Na^+ at 5.8%. Thermogravimetric analysis (TGA) data show a 16% weight loss for treatment to $600^\circ C$ with an 11% loss until about $300^\circ C$ and a gradual second loss starting at $400^\circ C$ to $600^\circ C$. Total loss of OH corresponds to a 17% weight loss. Two endotherms are observed at $190^\circ C$ and $325^\circ C$ in the differential scanning calorimetry (DSC) data. After the OL-2 samples are heated to $500^\circ C$, cooled to room temperature, and another DSC is run, no endotherms (or exotherms) are observed.

AC impedance measurements of OL-2 show values of $1.2 \times 10^{-6} \Omega^{-1}cm^{-1}$ at room temperature. Scanning electron microscopy data show that the particles have pseudo-cubic morphologies and are on the order of 10 μ . Energy dispersive X-ray (EDX) analyses are consistent with the atomic absorption analyses at least with respect to elements that are present and in relative compositions.

Fourier transform infrared (FTIR) data collected by diffuse reflectance techniques on OL-2 show a strong band at 3650 cm^{-1} and a broad band from 800 to 600 cm^{-1} . FTIR data after pyridine chemisorption show a very strong band at 1462 cm^{-1} , a broad band at 1500 cm^{-1} , a weak peak at 1590 cm^{-1} , and a weak shoulder at 1440 cm^{-1} .

DISCUSSION.

The XRD data for OL-2 are clearly indicative of a layer structure similar to that of feitknechtite. The presence of Mg^{2+} in the synthesis mixture has several effects. First of all, the enhanced intensity of the (002) reflection is indicative of

preferential orientation. The other observed reflections are indicative of feitknechtite. At longer synthesis times, OL-1 is produced. There is clearly a transformation in time of OL-2 into OL-1. This can occur by loss of H and an increase of average manganese oxidation state from 3.15 to 3.6. Oxygen in air is likely the cause of the oxidation of OL-2; Feitknecht et al. indeed reported air sensitivity of hydrohausmannite [3]. The layer structures of OL-1 and OL-2 are essentially the same and it is expected that the β -MnOOH form is a more likely precursor to synthetic birnessite (OL-1) than the other forms shown in Figure 1.

The AMOS data are consistent with Mg^{2+} incorporation in the framework of OL-2 and the concomitant charge balance of Na^+ cations. These AMOS and elemental analysis data are consistent with observed incorporation of Mg^{2+} in octahedral framework sites of OL-1, synthetic cryptomelane and OMS-1, synthetic todorokite. The EDX data are inherently less quantitative than data from atomic absorption experiments, however, there are no other species detected in EDX experiments besides Mn, Na, and Mg.

AC impedance measurements and the ease of collection of SEM data suggest that OL-2 is a semiconducting material. The increase in AMOS on transformation to OL-1 may be due to enhancement of anion vacancies, as earlier proposed on the basis of thermal desorption data [12,13]. Oxygen anion vacancies have been proposed to be responsible for the semiconducting behavior of OMS and OL materials [10].

The FTIR data for OL-2 show a strong band at 3650 cm^{-1} which is due to OH groups. The broad band from 800 to 600 cm^{-1} is due to $Mn(O)_6-x(OH)_x$ groups having octahedral symmetry. FTIR data after pyridine chemisorption showing a very strong band at 1462 cm^{-1} are indicative of both Brønsted and Lewis acid sites. The broad band at 1500 cm^{-1} , is due to both Brønsted and Lewis acid sites. The weak peak at 1590 cm^{-1} , may be due to Brønsted acid sites. The weak shoulder at 1440 cm^{-1} is due to Lewis acid sites. All these bands appear to be shifted to higher frequencies than for other acidic materials [8,9].

The thermal stability data of TGA and DSC experiments show a 16% weight loss for treatment to 600°C . This is consistent with loss of the OH groups due to condensation reactions. The first weight loss up to about 300°C is due to conversion to Mn_2O_3 . The second loss starting at 400°C to 600°C is due to a conversion to manganosite, MnO. This is due to reduction to Mn^{2+} which occurs with most OMS and OL materials at various temperatures depending on the composition and structure of the material.

The two endotherms observed at 190°C and 325°C are consistent with these transformations as well as a conversion to OL-1 (at least partially under these conditions). After the OL-2 samples are heated to 500°C and cooled to room temperature, no endotherms (or exotherms) are observed after another DSC is run because the material has been irreversibly changed due to loss of OH groups.

The observation of a pseudo-cubic morphology is different from the hexagonal plate morphology of feitknechtite [3,7]. It is possible that the incorporation of Mg^{2+} in the framework of OL-2 causes a change in morphology

Fig. 2 Interconversion of OL-2 to OL-1



of the crystallites. The change in morphology of OL-2 with respect to natural feitknechtite is also similar to changes in morphology of doped (Mg^{2+} , Cu^{2+} , Ni^{2+} , Zn^{2+}) synthetic todorokite (OMS-1) materials [14] with respect to natural todorokite samples.

Exchange of Mg^{2+} and framework incorporation in octahedral sites of various clays [15], and octahedral layer structures like birnessite [16], and octahedral molecular sieve materials like synthetic todorokite [17] are consistent with several other reports in the literature [15-17].

CONCLUSIONS

The structural (XRD), compositional (AA, AMOS), thermal (TGA, DSC), morphological (SEM), functional group (FTIR), and acidity (pyridine FTIR) data discussed above are consistent with the formation of a layered feitknechtite structure that has Mg^{2+} framework substitution. The synthetic data reported here suggest that synthetic feitknechtite (OL-2) is initially formed at very short periods of time (20 min) in such experiments. At longer periods of time (20 min to 1.5 days) OL-2 converts to synthetic OL-1 via oxidation with air and incorporation of exchangeable cations in the interlayer spacing of OL-1, in order to maintain a charge balance in the system. The conversion of OL-2 to OL-1 is the most reasonable one based on the structures of various manganese oxyhydroxides. AC impedance measurements show that OL-2 is a semiconducting material, albeit a poor one. This is likely due to the limited mixed valency of OL-2 with other materials like OL-1, OMS-1, and OMS-2. The acidity measurements suggest that OL-2 might be used in acid catalyzed reactions especially at low temperatures. The role of Mg^{2+} may be to stabilize OL-2 via tighter binding of O^{2-} ions than with the OL-2 without Mg^{2+} . The longterm stability of OL-2 is still under investigation. However, oxidizing environments lead to the interconversion to OL-1 and other materials.

ACKNOWLEDGMENTS

This research was supported by the US Department of Energy, Office of Basic Energy Sciences, Division of Chemical Sciences. We thank Professor Stan Ching of Connecticut College for use of his atomic absorption apparatus.

REFERENCES

1. Feitknecht, V. W.; Marti, W. *Helv. Chem. Acta*, 1945, **28**, 129-148.

2. Frondel, C. Am. Min., 1953, 38, 761-769.
3. Feitknecht, V. W.; Brunner, P.; Oswald, H. R. Zeit. Anorg. Allgem. Chem., 1962, 316, 154-160.
4. Wells, A. F., Structural Inorganic Chemistry, 1973, 4th Edition, Pergamon Pres, Oxford, pp. 520-528.
5. Moore, T. E.; Ellis, M.; Selwood, P. W. J. Am. Chem. Soc., 1950, 72, 856-866.
6. Feitknecht, V. W.; Marti, W. Helv. Chem. Acta, 1945, 28, 148-156.
7. Bricker, O. Am. Min., 1965, 50, 1296-1354.
8. Shen, Y. F.; Zerger, R. P.; DeGuzman, R.; Suib, S. L.; McCurdy, L.; Potter, D. I.; O'Young, C. L. J. Chem. Soc. Chem. Comm., 1992, 17, 1213-1214.
9. Shen, Y. F.; Zerger, R. P.; DeGuzman, R.; Suib, S. L.; McCurdy, L.; Potter, D. I.; O'Young, C. L. Science, 1993, 260, 511-515.
10. DeGuzman, R. N.; Awaluddin, A.; Shen, Y. F.; Tian, Z. R.; Suib, S. L.; Ching, S.; O'Young, C. L. Chem. Mater., 1995, 7, 1286-1292.
11. Simon, M. W.; Nam, S. S.; Xu, W. Q.; Suib, S. L.; Edwards, J. C.; O'Young, C.-L. J. Phys. Chem., 1992, 96, 6381-6388.
12. Yin, Y. G.; Xu, W. Q.; DeGuzman, R.; Suib, S. L.; O'Young, C. L. Inorg. Chem., 1994, 33, 4384-4389.
13. Yin, Y. G.; Xu, W. Q.; Shen, Y. F.; Suib, S. L.; O'Young, C. L. Chem. Mater., 1994, 6, 1803-1808.
14. Shen, Y. F.; Suib, S. L.; O'Young, C. L. J. Am. Chem. Soc., 1994, 116, 11020-11029.
15. Berner, R. A. Principles of Chemical Sedimentology, McGraw-Hill, NY, 1971, 158-191.
16. Bach, S.; Periera-Ramos, J. P.; Baffier, N. J. Solid State Chem., 1990, 88, 325.
17. Golden, D. C.; Chen, C. C.; Dixon, J. B. Science, 1986, 231, 717-719.